Supplementary Figure Legends

Figure S1. Proliferation capacity of BM-, WAT- and UC- derived stromal cells. Data are shown as mean ± SD values over four passages done in duplicates of three independent donors (**A**) depicting total viable cell counts. (**B**) Cumulative population doublings have been calculated as ln(N)/ln(2) with N being the cell number of detached cells divided by the number of cells seeded. Two-way ANOVA with Tukey's multiple comparisons test was used to determine statistically significant differences (*p < 0.05, **p< 0.01, ***p< 0.001).

Figure S2. Clonogenicity of BM-, WAT- and UC- derived stromal cells. Data are shown as mean ± SD values of cloning efficiency [%] done in triplicates over four passages in HPL- and FBS-supplemented media with cells from three independent donors (*p < 0.05, **p< 0.01, ***p< 0.001, Two-way ANOVA with Tukey's multiple comparisons test). A seeding density of 1 MSC/cm² was used. Colony photographs from one representative donor per cell source are shown.

Figure S3. Flow cytometry immunophenotype. Representative histograms showing the surface marker expression of early passage stromal cells derived from bone marrow (BM; passage 0), white adipose tissue (WAT; passage 0) and umbilical cord (UC; passage 1) as indicated, expanded in HPL (red) and FBS (blue) supplemented medium are shown as overlays. IgG controls are displayed in black. One representative donor per source is presented.

Figure S4. *In vitro* differentiation capacity of BM-, WAT- and UC-derived stromal cells. Pictures shown are from one representative donor per source and culture medium as indicated. Total magnification 100x (scale bar: 100 µm) and 200x

(scale bar: 50 µm) adipogenic differentiation, negative control 100x (scale bar: 100 µm); 100x (scale bar: 500 µm) and 200x (scale bar: 200 µm) osteogenic differentiation, negative control 100x (scale bar: 500 µm); 40x (scale bar: 200 µm) and 200x (scale bar: 20 µm) chondrogenic differentiation, negative control 40x (scale bar: 200 µm).

Figure S5A. Tissue Factor (CD142) surface expression of stromal cells cultured in HPL- and FBS-supplemented media. Representative immunofluorescence images of BM, WAT and UC stromal cells as indicated. Cells were stained with DAPI (blue staining, nuclei) and anti-CD142-PE and enhanced with donkey anti-mouse-Alexa 568 antibody (red staining; tissue factor). Scale bars 50 µm.

Figure S5B. Flow cytometry analysis of tissue factor expression on BM-, WAT- and UC-derived stromal cells. Flow cytometry histograms show tissue factor expression overlays of stromal cells from the three different sources as indicated, cultured for two passages in HPL (red) and FBS (blue) supplemented media. IgG controls are displayed in black. Inserts show dot plots of sideward scatter signal plotted against TF staining to better illustrate the minor TF-positive sub-population that were present in HPL- as well as FBS-expanded BMSC; representative plots for HPL-expanded cells are depicted.

Figure S5C. Flow cytometry analysis of tissue factor expression on female BM stromal cells. Flow cytometry analysis of three additional female donor early passage HPL-expanded BMSC was performed as described in Figure S5B to question gender differences in TF expression. Representative plots for HPL-expanded cells are depicted.

Figure S6. Schematic illustration of plasma coagulation parameters measured by rotational thromboelastometry. In our test system using pooled human blood group AB plasma the clotting time (**CT**) indicates the time to initiate clot formation, defined as clot amplitude of 2 mm. Clot formation time (**CFT**; violet) represents the time between clot initiation (2 mm) and an amplitude of 20 mm, corresponding to thrombin formation under the aegis of coagulation factor Xa. The **α-angle** results from making a tangent between the clot initiation point (end of clotting time, 2 mm amplitude) to the slope of the amplitude. The α-angle corresponds to fibrin monomer deposition after thrombin formation. The mean clot firmness (**MCF**) represents the peak amplitude of the clot formed in this system. The picture is derived from measuring a randomly selected plasma sample. Thromboelastometry parameters are drawn based on www.rotem.de/en/methodology/rotem-delta-and-sigma-analysis/.

Figure S7. BMSC sorting strategy. A stringent sort strategy was devised to obtain highly pure TF^+ and TF-deficient BMSCs. (**A**) Cell size (forward scattering area, FSC-A) and granularity (side scatter area, SSC-A) were used to identify the main cell fraction. (**BC**) Two additional gates were used to exclude cell doublets as depicted (-H = signal heights) particularly to avoid contamination of the TF^+ fraction by TF-deficient BMSCs. (**D**) Stringent gates were set to identify TF^+ and TF-deficient BMSCs. Re-analysis of cells after sorting with a FACSAria III instrument revealed purity of both (**E**) the TF-deficient and (**F**) the TF^+ populations. One representative example out of three sorts of independent BMSCs is shown.

Figure S8. TF expression of sort-purified BMSCs after culture. Re-analysis of TF expression of purified TF^+ and TF^- BMSCs from three donors after one additional cell

culture passage to amplify the TF^+ cells showed app. 4.7–23% TF reactivity of previously purely positive and app. 0.5-1.8% reactivity of previously purely TF-negative cells.

Figure S9 – corresponding to Figure 7. Thromboembolic risk of systemically applied TF-depleted human BM compared to TF-expressing UC stromal cells. (**A**) A lower magnification of the same Masson's trichrome stained lung, liver and spleen sections as shown in Figure 7 is depicted derived from rats one hour after intravenous injection of 1.5 million TF-deficient sort-purified human BMSCs (BM TF^{DEF}; bottom row) or un-sorted human UC stromal cells (UC TF^{HIGH}; top row). Scale bar 100 µm. (**B**) Hematoxylin eosin staining illustrates leukocyte trapping in different sections obtained from rats one hour after injection of 1.5 million human BMSCs (BM TF^{DEF}; bottom row) or un-sorted human UC stromal cells (UC TF^{HIGH}; top row). Representative pictures are shown. Scale bar 100 µm.

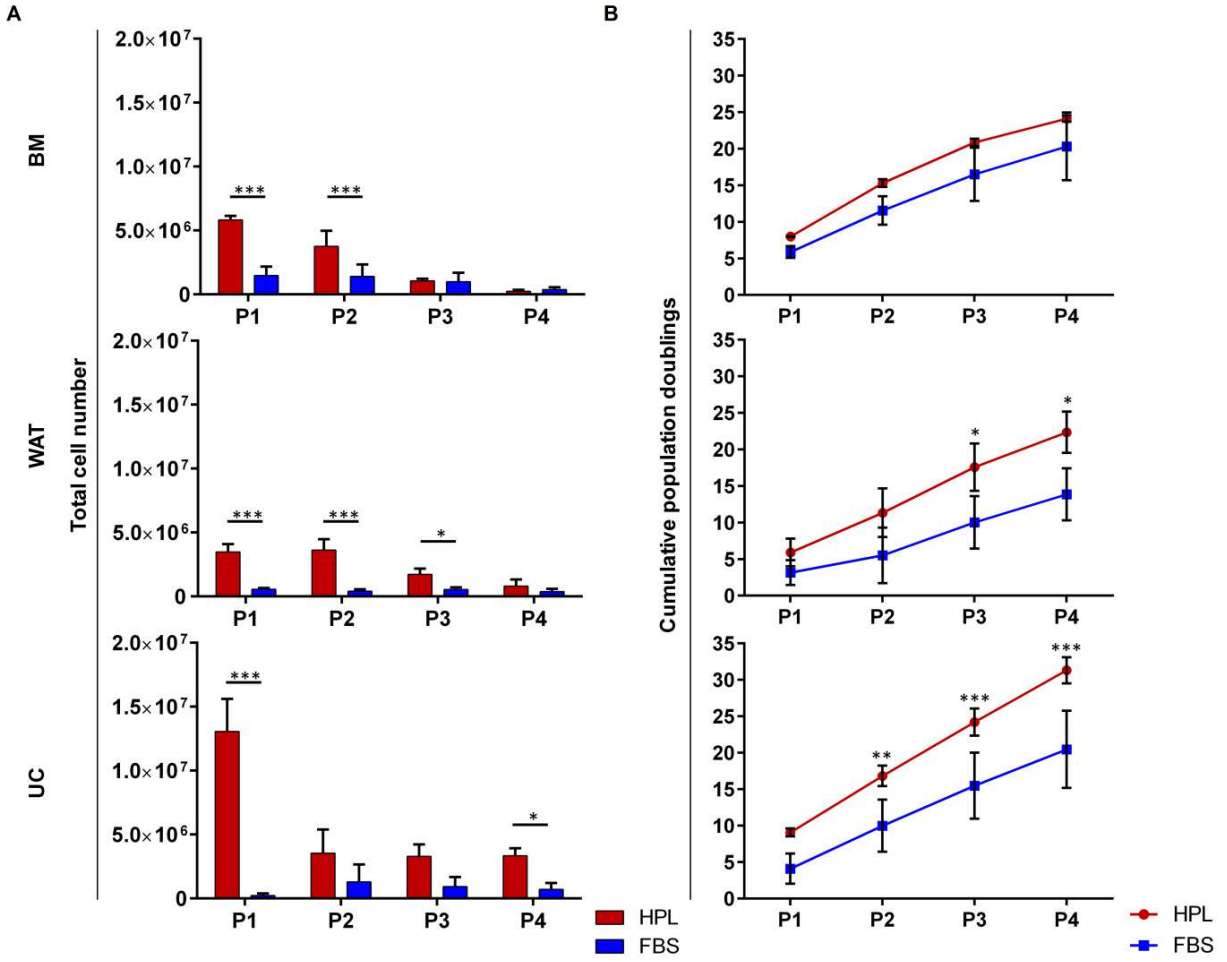

Figure S1

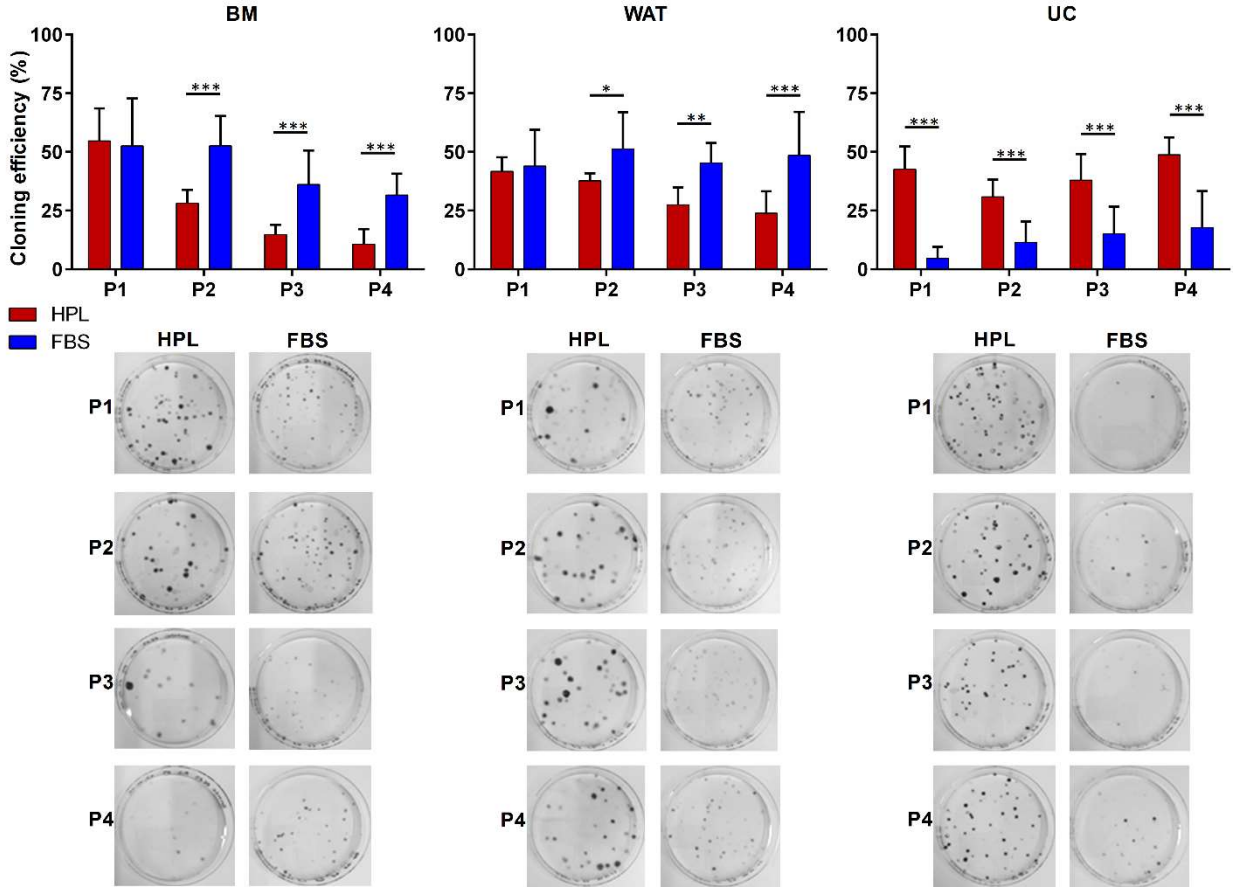

Figure S2

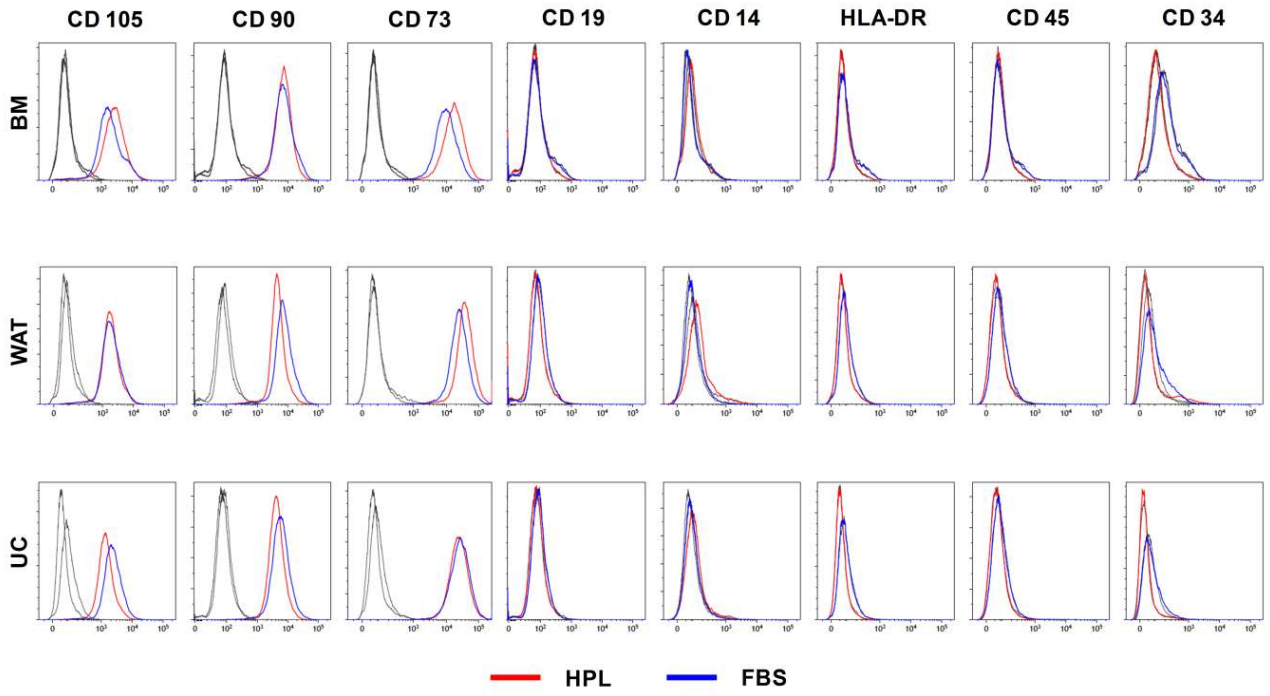

Figure S3

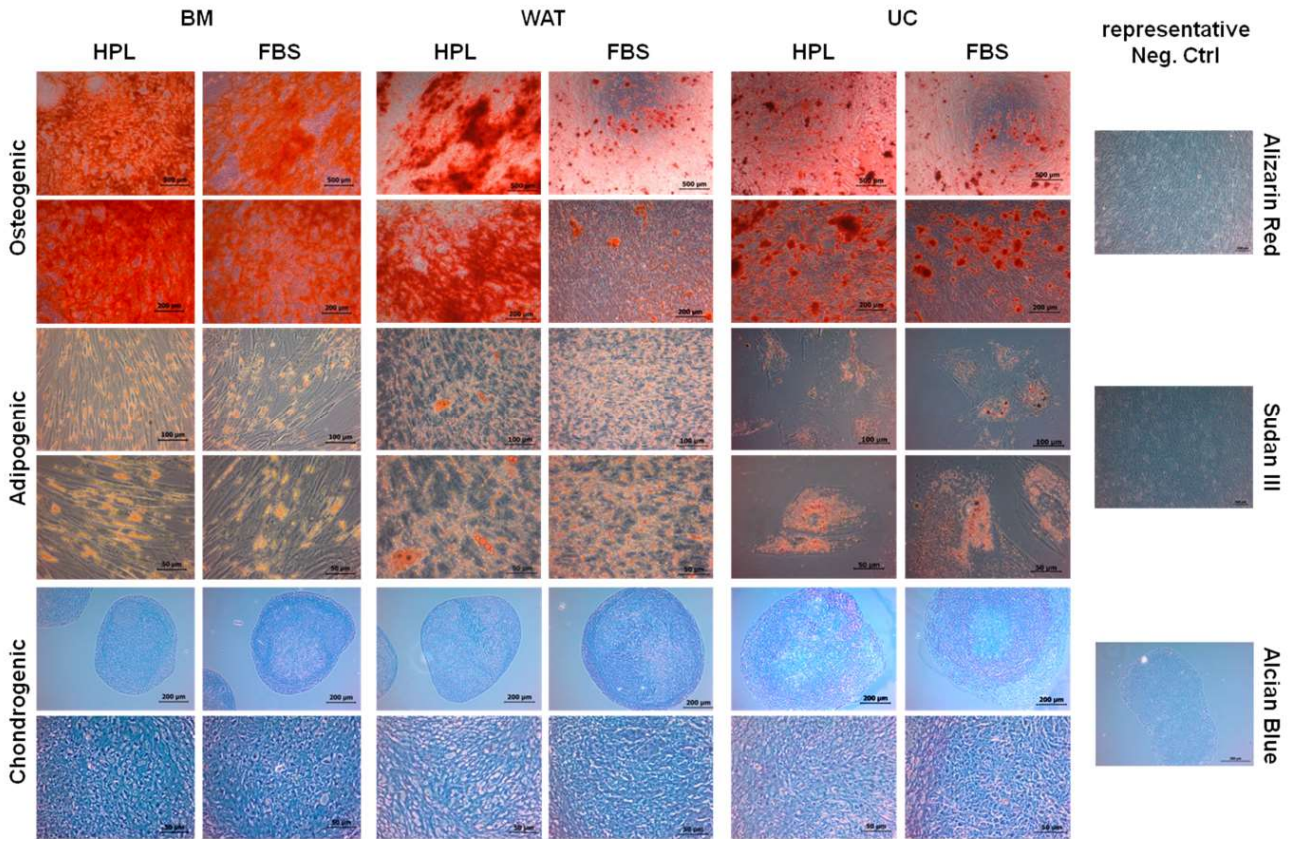

Figure S4

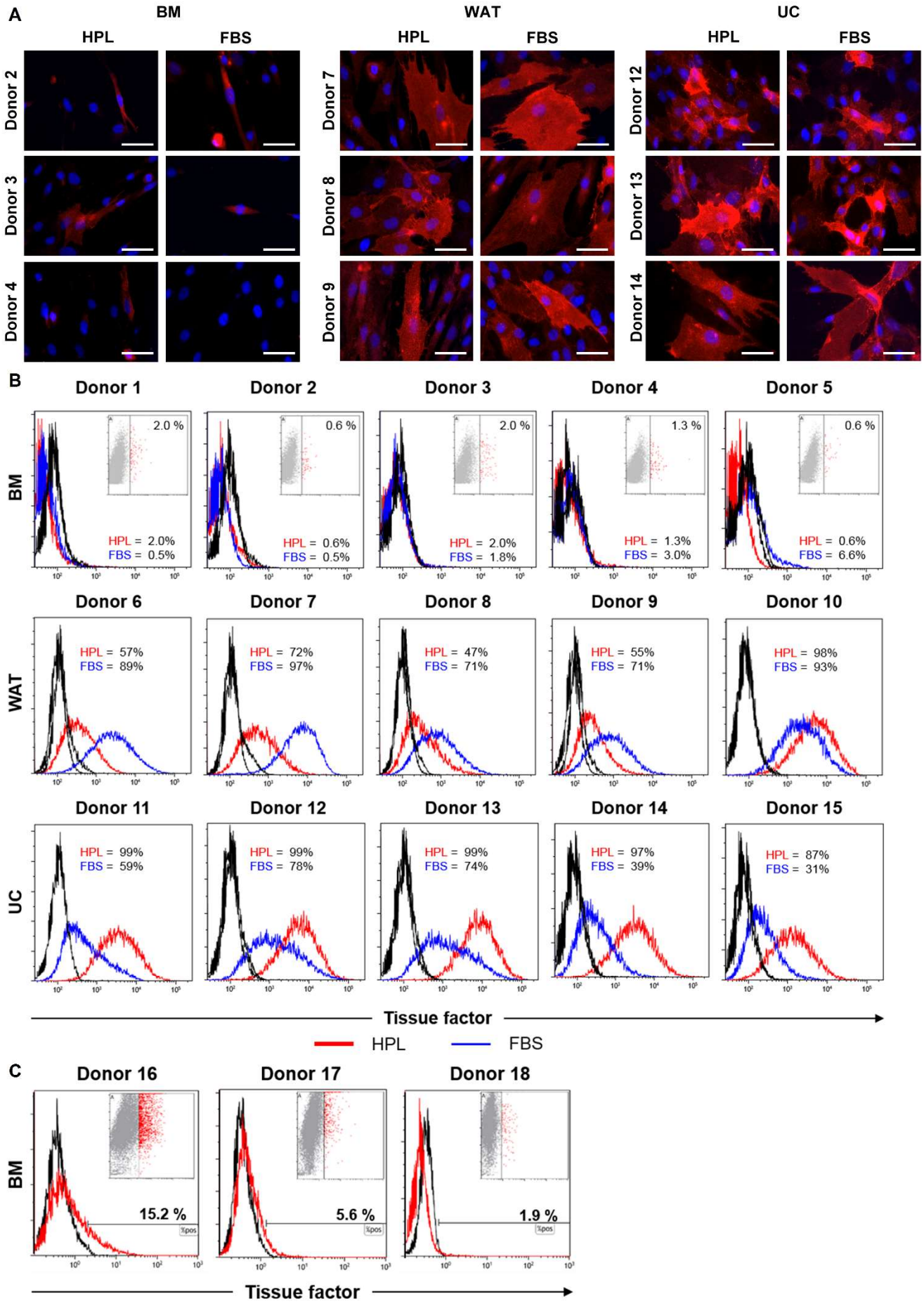
A
BM
WAT
UC
HPL
FBS
Donor 2
Donor 3
Donor 4
Donor 7
Donor 8
Donor 9
Donor 12
Donor 13
Donor 14
B
Donor 1
Donor 2
Donor 3
Donor 4
Donor 5
BM
2.0 %
0.6 %
2.0 %
1.3 %
0.6 %
HPL = 2.0%
FBS = 0.5%
HPL = 0.6%
FBS = 0.5%
HPL = 2.0%
FBS = 1.8%
HPL = 1.3%
FBS = 3.0%
HPL = 0.6%
FBS = 6.6%
Donor 6
Donor 7
Donor 8
Donor 9
Donor 10
WAT
HPL = 57%
FBS = 89%
HPL = 72%
FBS = 97%
HPL = 47%
FBS = 71%
HPL = 55%
FBS = 71%
HPL = 98%
FBS = 93%
Donor 11
Donor 12
Donor 13
Donor 14
Donor 15
UC
HPL = 99%
FBS = 59%
HPL = 99%
FBS = 78%
HPL = 99%
FBS = 74%
HPL = 97%
FBS = 39%
HPL = 87%
FBS = 31%
Tissue factor
HPL
FBS
C
Donor 16
Donor 17
Donor 18
BM
15.2 %
5.6 %
1.9 %
Tissue factor

Figure S5

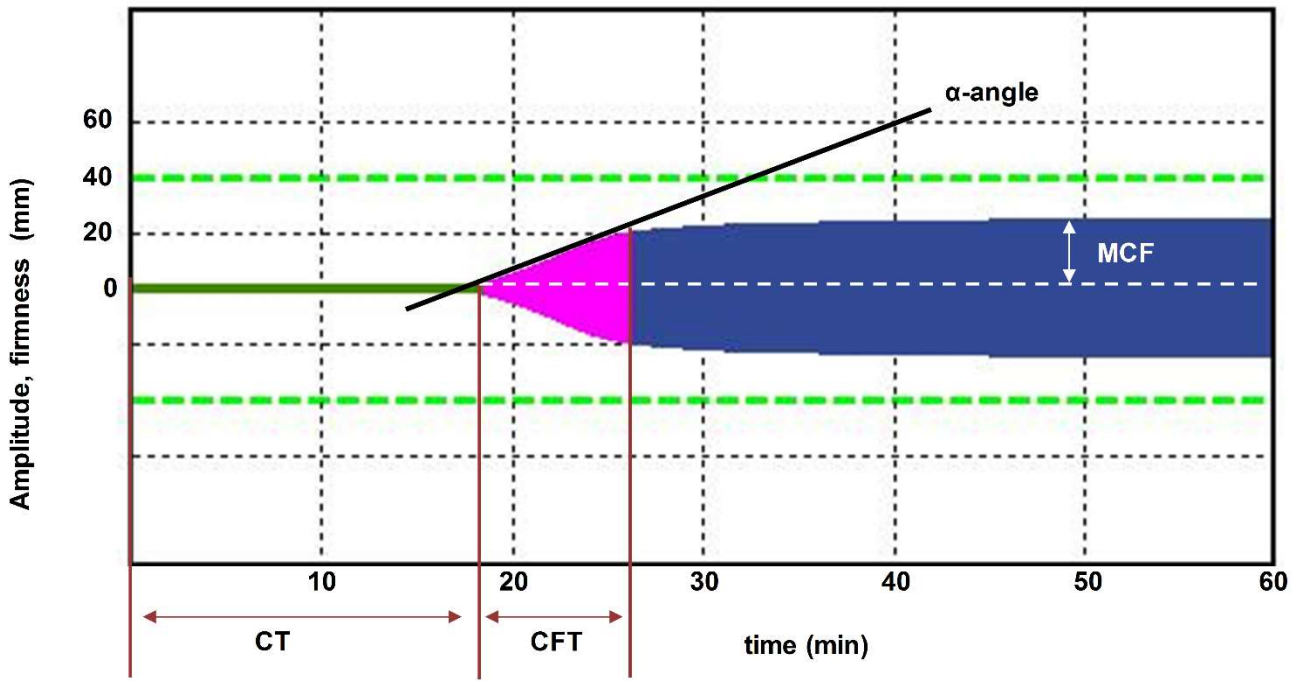

Figure S6

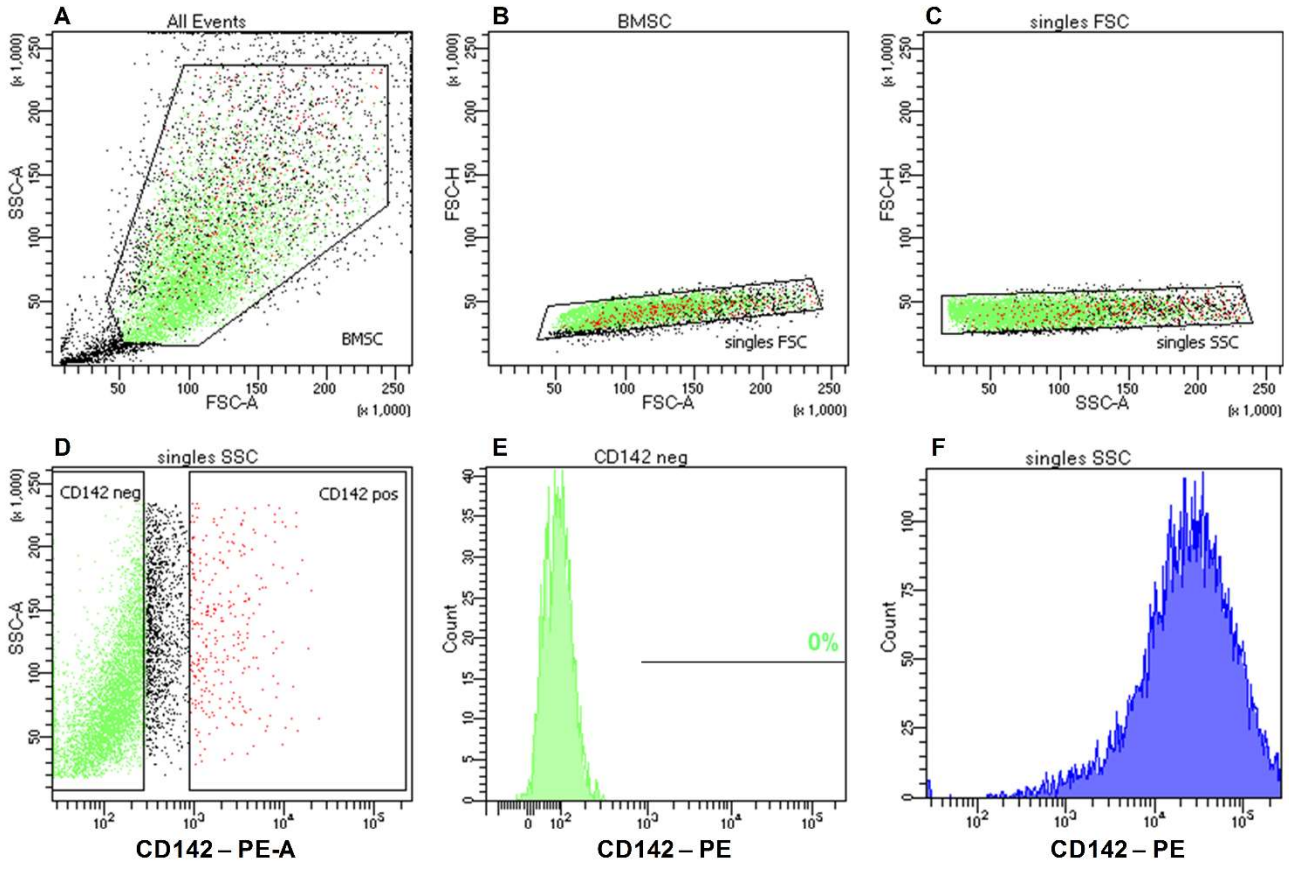

Figure S7

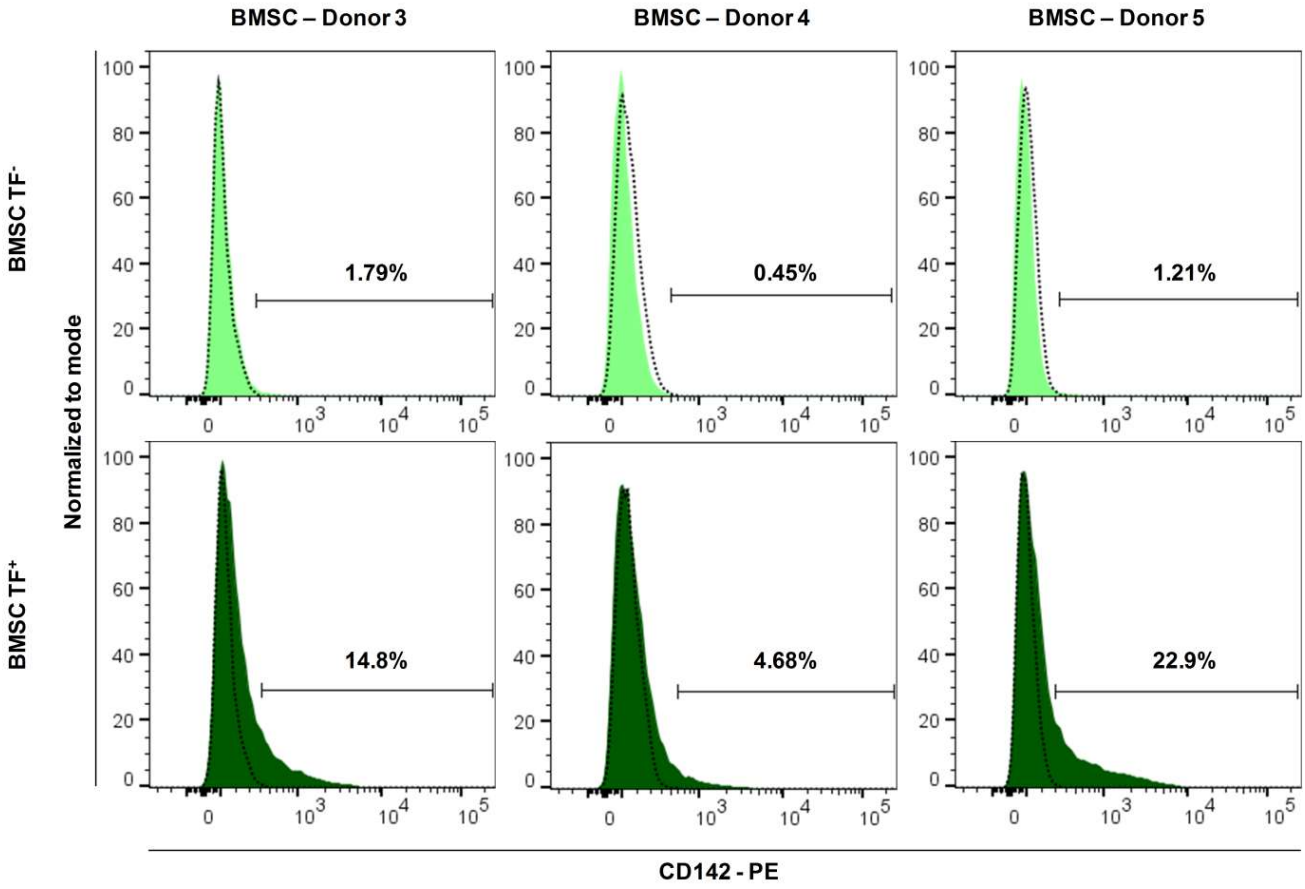
BMSC – Donor 3
BMSC – Donor 4
BMSC – Donor 5
BMSC TF-
BMSC TF+
Normalized to mode
1.79%
0.45%
1.21%
14.8%
4.68%
22.9%
CD142 - PE

Figure S8

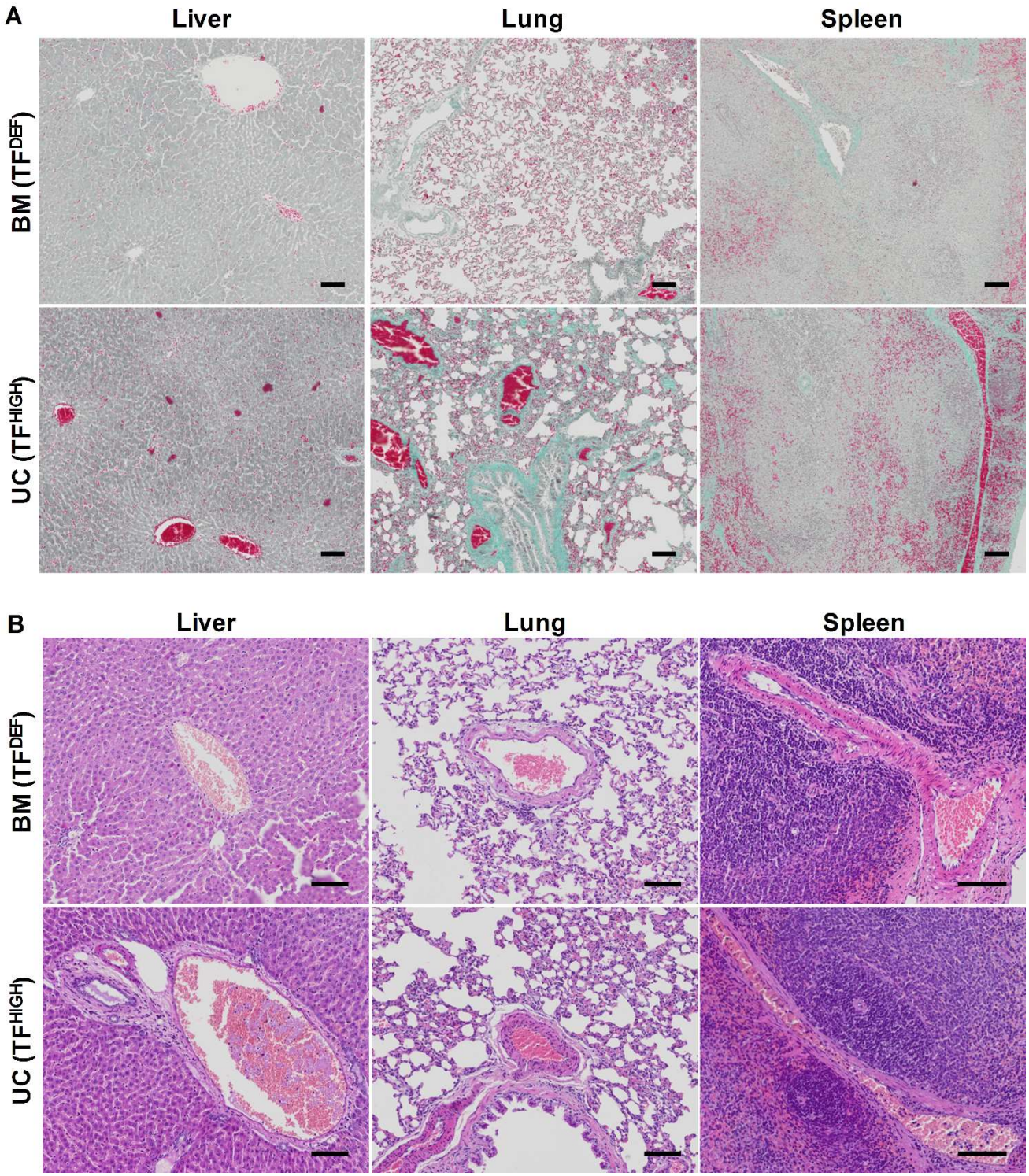
A
Liver
Lung
Spleen
BM (TF^DEF)
UC (TF^HIGH)
B
Liver
Lung
Spleen
BM (TF^DEF)
UC (TF^HIGH)

Figure S9